

Two-level Dynamic Load Balancing for High Performance Scientific Applications

Ali Mohammed¹, Aurélien Cavelan¹, Florina M. Ciorba¹, Rubén M. Cabezón²
and Ioana Banicesu³

¹Department of Mathematics and Computer Science, University of Basel,
Switzerland,

² Scientific Computing Center (sciCORE), Department of Physics, University of
Basel, Switzerland

³ Department of Computer Science and Engineering, Mississippi State
University, USA

November 18, 2019

Contents

1	Introduction	4
2	Background and Related Work	5
2.1	Background	6
2.1.1	Self-scheduling	6
2.1.2	DLS implementation in MPI and OpenMP	7
2.1.3	Single-level dynamic load balancing	7
2.2	Related Work	7
3	Two-level Dynamic Load Balancing	8
3.1	Implementation	9
3.2	Execution	10
4	Performance Evaluation and Discussion	12
4.1	Design of Experiments	12
4.1.1	Applications	12
4.1.2	Two-level dynamic load balancing	18
4.1.3	Computing systems	18
4.2	Experimental Results	18
4.3	Discussion	23
5	Conclusion and Future Work	24

Abstract

Scientific applications are often complex, irregular, and computationally-intensive. To accommodate the ever-increasing computational demands of scientific applications, high performance computing (HPC) systems have become larger and more complex, offering parallelism at multiple levels (e.g., nodes, cores per node, threads per core). Scientific applications need to exploit *all* the available multilevel hardware parallelism to harness the available computational power. The performance of applications executing on such HPC systems may adversely be affected by load imbalance at multiple levels, caused by problem, algorithmic, and systemic characteristics. Nevertheless, most existing load balancing methods do not simultaneously address load imbalance at multiple levels. This work investigates the impact of load imbalance on the performance of three scientific applications at the thread and process levels. *We jointly apply and evaluate selected dynamic loop self-scheduling (DLS) techniques to both levels.* Specifically, we employ the extended LaPeSD OpenMP runtime library [1] at the thread level, and extend the *DLS4LB* MPI-based dynamic load balancing library [2] at the process level. This approach is generic and applicable to any multiprocess-multithreaded computationally-intensive application (programmed using MPI and OpenMP). We conduct an exhaustive set of experiments to assess and compare six DLS techniques at the thread level and eleven at the process level. The results show that improved application performance, by up to 21%, can only be achieved by *jointly* addressing load imbalance at the two levels. We offer insights into the performance of the selected DLS techniques and discuss the interplay of load balancing at the thread level and process level.

Keywords.

Two-level dynamic load balancing, Computationally-intensive applications, High performance computing, Self-scheduling, MPI+OpenMP

1 Introduction

Scientific applications are typically large, irregular, and computationally-intensive. To match the ever-increasing computational demands of scientific applications, high performance computing (HPC) systems have become larger and more complex. Not only the number of compute nodes in an HPC system has increased, but also the number of CPU sockets and the number of cores per socket have increased. For example, the number of CPU cores per node in the top 3 supercomputing systems¹ is ranging from 44 to 260 cores. Therefore, applications need to exploit hardware parallelism at multiple levels to achieve the best performance.

Due to the hybrid nature of current HPC systems, distributed memory across compute nodes and shared memory within a single node, hybrid parallelization of applications at process level and thread level using MPI+OpenMP is the most common and successful approach in scientific applications [3–5]. However, the performance of scientific applications on such systems may be degraded due to load imbalance. Load imbalance can be caused by irregular application or computing system characteristics, such as conditional statements leading to the variation of computations and non-uniform memory access latency, respectively. Load imbalance degrades application performance and hinders its scalability. To balance the load among parallel processes, several scientific applications use domain decomposition methods, such as octagonal recursive bisection (ORB) [6]. However, the computational load per sub-domain may change as the execution evolves and causes imbalance. Also, these methods can not adapt to the load imbalance due to system characteristics, such as non-uniform memory accesses (NUMA) and perturbations. Other applications, such as ChaNGa [7], rely on load balancing solutions offered by specific programming abstractions (Charm++)². In addition, applications, such as Lassen, Kripke, and ChaNGa, create OpenMP tasks to help overloaded chares (in Charm++) to balance the load among processing elements (PEs) in a shared memory domain [8]. Also, as the number of PEs in a shared memory domain has increased, the standard OpenMP scheduling options may not be sufficient to achieve a balanced load execution [1].

Moreover, load imbalance may manifest in more than one level of software parallelism, i.e., among processes (process-level) and among threads (thread-level). For example, Figure 1 conceptually shows the two-level load imbalance of a scientific application parallelized using multiple processes and threads. Due to the thread level load imbalance, threads that finish early must wait until the slowest thread finishes (yellow regions). Therefore, the performance of a process is dominated by its slowest thread. Similarly, at the process level, the faster process has to wait for the slower one and the application performance is dominated by its slowest process. The two-level load imbalance is a compound problem and not trivial to address as the scheduling performance at one level is influenced by the scheduling decisions at the other. For example, the relation between batch and application level scheduling was studied [9], and it was shown that a holistic solution results in better performance improvement than focusing on improving the performance at each level alone.

In this work, dynamic load balancing via dynamic loop self-scheduling (DLS) is jointly applied at both the thread- and the process-levels to achieve improved performance. DLS self-schedules groups of loop iterations (tasks), or chunks, to free and requesting PEs, e.g., processes or threads, to achieve a dynamically balanced load execution. DLS techniques have successfully been

¹<https://www.top500.org/lists/2018/11/>

²<http://charm.cs.illinois.edu/research/charm>

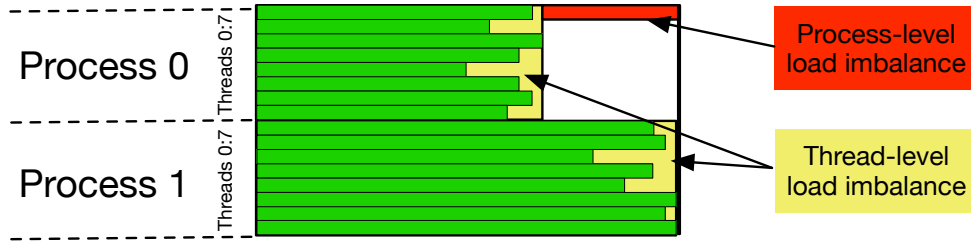


Figure 1: Conceptual illustration of the impact of the two-level load imbalance of a scientific application on two processes each with eight threads. Due to the uneven load at the thread level, faster threads wait for the slowest thread in each process, represented by the yellow regions. At the process level, process 0 (faster) waits for process 1 (slower), represented by the red region. The application completes when the slower process (process 1) finishes.

used to achieve load balance in computationally-intensive scientific applications, such as heat diffusion [10], wave packet simulations [11], and N-Body simulations [12]. The DLS techniques are generic and have been implemented in various programming models. In this work, they are applied at the thread- and the process-levels to three scientific applications, Mandelbrot [13], PSIA [14], and SPHYNX [15]. DLS techniques are applied to the three applications at the thread level using an extended version of the GNU OpenMP runtime time library [1] (*eLaPeSD*), and at the process level using an extended version of the *DLS4LB* [2]. Sixty six combinations of DLS techniques at the thread and the process levels are explored to find the best combination of DLS techniques at both levels for the applications of interest.

This work makes the following contributions: (1) A generic approach of two-level dynamic load balancing using DLS techniques with *eLaPeSD* at the thread level, and the extended *DLS4LB* at the process level; (2) The extension of the *DLS4LB* [2] with the adaptive weighted factoring (AWF) technique that supports time-stepping applications; the modification of the AWF variants namely AWF-B, C, D, E to share the learned updated weights between time-steps; (3) The analysis of the two-level load imbalance in three scientific applications and its impact on performance; (4) Exhaustive scheduling experiments that test different combinations of thread level and process level scheduling techniques that led to the performance enhancement of applications up to 21%; (5) Insights into the performance of the selected DLS techniques and the interplay of load balancing at the thread level and process level.

This work is structured as follows: Section 2 contains a brief review of self-scheduling techniques, as well as of the work related to the load balancing in the literature and the use of DLS techniques to balance the load of scientific applications. The proposed methodology of using DLS techniques to load balance at the two (thread and process) levels is explained in Section 3. The experimental design and setup and the performance of the proposed approach are described and discussed in Section 4. The work concludes and outlines potential future work in Section 5.

2 Background and Related Work

A brief background on self-scheduling techniques is presented in this section. Besides, load balancing libraries and the applied load balancing methods to scientific applications are discussed.

2.1 Background

2.1.1 Self-scheduling The iterations of computationally-intensive loops or tasks are assigned to PEs to achieve a balanced load execution with minimum overhead. Loop scheduling techniques are divided into static and dynamic. In this work, block scheduling is considered, denoted as STATIC, where each PE is assigned a block or chunk of tasks equal to the number of tasks, N , divided by the number of PEs, P . DLS techniques assign a chunk of tasks to free and requesting PEs during execution via *self-scheduling*. Self-scheduling is different from *work stealing* [16] where PEs are initially assigned a block of tasks and they need to steal afterward from distributed work queues to balance the load, whereas in self-scheduling tasks are only assigned to free and requesting PEs from a central work queue. The DLS techniques can further be divided into nonadaptive and adaptive techniques. The nonadaptive DLS techniques address the load imbalance caused by problem or application characteristics, such as the variation of tasks execution times. Nonadaptive DLS techniques include self scheduling [17] (SS), fixed-sized chunking [18] (FSC), modified fixed-sized chunking [19] (mFSC), guided self-scheduling [20] (GSS), trapezoid self-scheduling [21] (TSS), factoring [22] (FAC), weighted factoring [23] (WF), and random [1] (RAND). SS assigns a single loop iteration at a time per PE request. Thus, it results in the maximum load balance and the maximum scheduling overhead. SS represents one extreme, where the load balancing effect and the scheduling overhead are at maximum, whereas STATIC represents the other extreme, where load balancing effect and the scheduling overhead are at minimum. FSC assigns loop iterations in chunks of fixed size, hence reducing the scheduling overhead compared to SS. The chunk size depends on the scheduling overhead, h , and the standard deviation of the iterations execution time, σ . mFSC alleviates the burden of determining h and σ and assigns a chunk size that results in a number of chunks that is similar to that of FAC (explained below). GSS addresses the uneven starting times of PEs and assigns chunks in decreasing sizes. The chunk sizes in GSS are calculated as the number of the remaining loop iterations, R , divided by P . TSS assigns chunks of decreasing sizes, similar to GSS. However, chunk sizes decrease linearly in TSS, which simplifies the chunk calculation and reduces scheduling overhead. FAC assigns chunks in batches to reduce the scheduling overhead. FAC employs probabilistic analysis of application characteristics to calculate batch sizes that maximize the probability of achieving a balanced load execution. The batch size calculation depends on the mean of iterations execution times, μ , and their standard deviation, σ . The chunk sizes are equal in a batch, namely the batch size divided by P . When μ and σ are not available, FAC is practically implemented by assigning half of the remaining loop iterations as a batch, which is equally distributed to PEs on request. WF is similar to FAC, except that it addresses heterogeneous PEs. In WF, each PE is assigned a relative weight that is fixed during execution. Each PE is assigned a chunk from the current batch relative to its weight. In this work, the practical implementations of FAC and WF are used. RAND employs the uniform distribution to arrive at a randomly calculated chunk size between an upper and a lower bound. The randomly calculated chunk size is bounded by $N/(100 \times P) \leq chunk_size \leq N/(2 \times P)$ [1]. The adaptive DLS techniques measure the performance during execution and adapt their chunk calculation accordingly to address the load imbalance due to systemic characteristics, such as non-uniform memory access (NUMA) delays and perturbations during execution. The adaptive DLS techniques include adaptive weighted factoring [24] (AWF), its variants [11] AWF-B, AWF-

C, AWF-D, AWF-E, and adaptive factoring [25] (AF), among others. AWF adapts the relative PE weights during execution according to their performance. It is designed for time-stepping applications. It measures the performance of PEs during previous time-steps and updates the PEs relative weights after each time-step to balance the load according to the computing system's present state. AWF-B relieves the time-stepping requirement to learn the PE weights. It learns the PE weights from their performance in previous batches instead of time-steps. AWF-C is similar to AWF-B, however, the PE weights are updated after the execution of each chunk, instead of batch. AWF-D is similar to AWF-B, where the scheduling overhead (time taken to assign a chunk of loop iterations) is taken into account in the weight calculation. AWF-E is similar to AWF-C, and takes into account also the scheduling overhead, similar to AWF-D. AF is also based on FAC. However, it measures the performance of PEs to learn the μ and σ per PE during execution.

2.1.2 DLS implementation in MPI and OpenMP A dynamic load balancing tool (*DLB_tool*) that implements certain DLS techniques at the process level using MPI was introduced and used to balance the load of an image denoising model and at the simulation of a vector functional coefficient autoregressive (VFCAR) model for multivariate nonlinear time series [26]. The *DLB_tool* initially implemented nine loop scheduling techniques: STATIC, mFSC, GSS, FAC, AWF-B, AWF-C, AWF-D, AWF-E, and AF. The *DLB_tool* employ self-scheduling and use a master-worker execution model. Free MPI processes request work from the master process that executes the self-scheduling techniques. The master also doubles as a worker process and executes chunks of tasks. The *DLB_tool* was further extended into *DLS4LB* [2] with four additional DLS techniques: SS, FSC, TSS, and WF to support 13 DLS techniques in total, and was used to balance the load of two scientific applications (PSIA [27] and Mandelbrot [13]) and five synthetic workloads.

At the thread level scheduling, the GNU OpenMP runtime library was extended into *eLaPeSD* [1] to support four additional DLS techniques: FSC, TSS, FAC, and RAND in addition to the standard OpenMP scheduling techniques: STATIC, dynamic (actually SS [17]), and guided (actually GSS [20]).

2.1.3 Single-level dynamic load balancing DLS techniques have been used in several studies to improve the performance of computationally-intensive scientific applications at a single software parallelism level: process level. For example, SS, FAC, AWF, and AF were used to balance the load of a heat conduction application on an unstructured grid [10]. AF was found to result in a superior performance, especially with irregular applications executing in heterogeneous environments. The DLS techniques were used to balance the load of scientific applications, such as simulations of wave packet dynamics, N-Body simulations [12], automatic quadrature routines [11], and a computer vision application (PSIA) [27]. The DLS techniques were also used to balance the load of scientific benchmarks, such as NAS parallel [28] and RODINIA [29] benchmarks, at the thread level [1]. This work is the first to jointly explore the use of the DLS techniques at both process- and thread-levels.

2.2 Related Work A hierarchical domain decomposition using space-filling curves was introduced to achieve a balanced load execution of an atmospheric cloud model [30]. The division

of the space-filling curve and the assignment of each part are performed in two stages using an exact algorithm and a heuristic to reduce the complexity of the curve cutting problem to achieve load balancing with low overhead. However, the above work used hierarchical scheduling to simplify the scheduling problem at a single software parallelism level. Hierarchical scheduling has been used also at the thread level for the scheduling on multicore hyper-threaded CPUs, where the first level of the hierarchical scheduling is for scheduling work to the cores, and the second level is for scheduling and load balancing between hyper threads that share the same core. However, no interaction between the scheduling on the two levels were considered or studied and only studied hierarchical scheduling within one level of parallelism, i.e. thread level. Quo [31] was introduced to adapt threads and processes binding during runtime to improve MPI+OpenMP applications performance. Quo adapts processes/threads bindings to PEs to accommodate the newly spawned/suspended threads during different computational phases within an application and preserve data locality. However, an overloaded thread or process may still cause load imbalance at the thread level or the process level. ChaNGa [7] uses over-decomposition, supported by Charm++, to allow fine and dynamic load balancing of chares execution among PEs. Load statistics are collected, and particles are migrated between the PEs to balance the load [32]. OpenMP was integrated with Charm++ to balance the load among PEs in a shared memory domain in applications, such as Lassen, Kripke, and ChaNGa [8] by creating OpenMP tasks to help overloaded chares. Adaptive hierarchical scheduling [33] (AHS) was proposed for the two-level scheduling on multi-core clusters. The work is initially divided between the nodes with the aim to achieve a balanced load among them. Work-stealing was used for intra-node load balancing between the threads whereas both work-stealing and work-sharing were used for inter-node load balancing.

Load balancing solutions based on domain decomposition can not adapt to accommodate all (unpredictable) variations in the computing system characteristics. Balancing solutions that are language-specific, such as Charm++, can not easily be ported to other scientific applications. None of the efforts mentioned above analyzed the effects of two-level (process and thread) load imbalance nor studied the benefits of load balancing at one of the levels on the other level.

This work studies load imbalance at the thread level and the process level in 3 scientific applications; PSIA [14], Mandelbrot [13], and SPHYNX [15]. The *eLaPeSD* is used to balance the load at the thread level and the *DLS4LB* [2] to support the AWF DLS technique (that supports time-stepping applications, such as SPHYNX in this work), to balance the load at the process level. Moreover, adaptive DLS techniques, such as the AWF-B, AWF-C, AWF-D, and AWF-E are improved such that the learned updated PE weights are transferred from previous time-steps to the current time-step, to support time-stepping applications, such as SPHYNX. Sixty six joint combinations of DLS techniques at the thread level and the process level are tested to achieve the best performance for the three scientific applications.

3 Two-level Dynamic Load Balancing

Addressing load imbalance at both the process and the thread levels is essential to achieve improved application performance. Figure 2 describes the proposed two-level dynamic load balancing via self-scheduled approach. At the process level, the *DLS4LB* self-schedules a chunk of tasks to a free and requesting MPI rank in multiple rounds. The work assigned to an MPI rank is parallelized and distributed among several OpenMP threads (8 threads per rank) using the

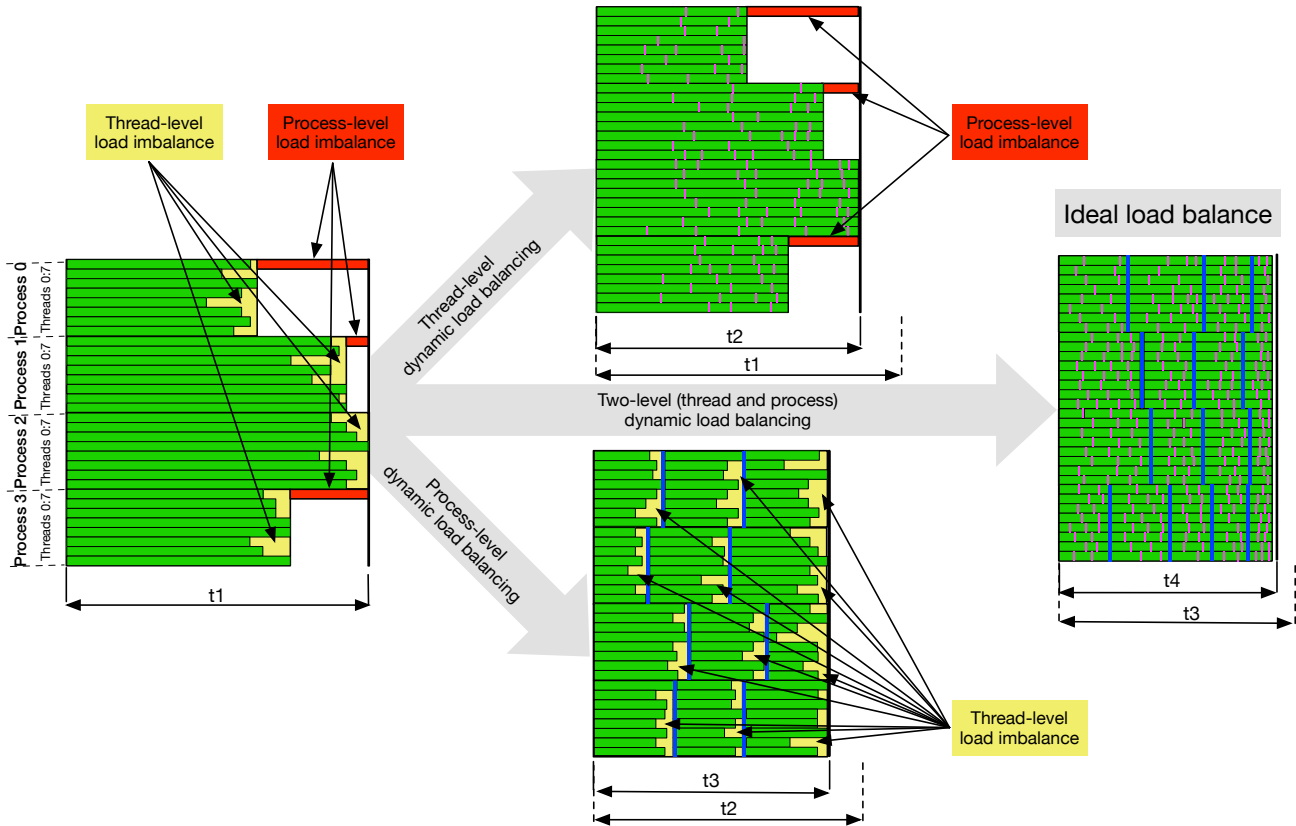


Figure 2: Conceptual illustration of employing two-level dynamic load balancing via *eLaPeSD* and *DLS4LB*. At the thread level, OpenMP threads are self-scheduled chunks of tasks using the extended GNU runtime library *eLaPeSD*. At the process level, the *DLS4LB* self-schedules chunks of tasks to free and requesting MPI ranks in multiple rounds.

eLaPeSD OpenMP runtime library for load balancing. The library self-schedules a chunk of tasks (a subset of the loop iterations assigned to this MPI rank at the process level by the *DLS4LB*) to a free and requesting thread. Employing DLS at only one level (either process level or thread level) achieves load balance at this level and improves the application performance as shown in the middle subplots in Figure 2. However, the best application performance can only be achieved by employing dynamic load balancing at the two levels as shown in Figure 2. Based on the selected DLS technique at the thread level via the `OMP_SCHEDULE` environment variable, and the selected scheduling technique at the process level, via the *DLS4LB*, along with the application and the computing system properties, different degrees of load balancing and performance improvement are achieved as shown in Section 4. The two-level dynamic load balancing approach proposed and depicted in Figure 2 is generic and can be used with any scientific application parallelized with MPI+OpenMP hybrid parallelization.

3.1 Implementation To balance the load at the thread level, an extended version of GNU OpenMP runtime library LaPeSD, i.e., *eLaPeSD* [1] is used. *eLaPeSD* supports seven OpenMP scheduling techniques that can be selected by exporting the name of the scheduling technique to

the OpenMP environment variable `OMP_SCHEDULE`. Recall that *eLaPeSD* provides four additional dynamic loop scheduling techniques, FSC, TSS, FAC, and RAND in addition to the three original OpenMP scheduling techniques: static, dynamic, and guided. The OpenMP static scheduling clause corresponds to the STATIC technique, where each thread is assigned only one chunk of size N/P . The dynamic and guided scheduling clauses correspond to SS and GSS, respectively (c.f. Section 2). To enable the application to read and use scheduling algorithms defined in the OpenMP runtime library, `schedule(runtime)` needs to be added to the OpenMP parallelization of a for loop (in C) or a do loop (in FORTRAN), as shown in Listing 1 Line 21 (line in magenta font color). The path to the *eLaPeSD* library needs to be added to the dynamic library path variable `LD_LIBRARY_PATH` to call our extended OpenMP runtime library instead of the standard one. Currently, our extended library only works with GNU compilers, while an extended LLVM OpenMP runtime library is currently under development.

To balance the load at the process level, our extended *DLS4LB* is used to dynamically distribute the application tasks to MPI ranks in multiple rounds via self-scheduling. Recall that the *DLS4LB* provides 13 loop scheduling techniques, ranging from fully static to fully dynamic, nonadaptive and adaptive, namely: STATIC, SS, FSC, mFSC, TSS, GSS, FAC, WF, AWF-B, AWF-C, AWF-D, AWF-E, and AF (c.f. Section 2). In this work, it is extended to support an additional DLS technique; the AWF originally developed for time-stepping applications [24]. This is needed due to the time-stepping nature of scientific simulations, such as SPHYNX. Moreover, AWF-B, AWF-C, AWF-D, and AWF-E are improved to share the learned updated PE weights between time-steps, instead of starting with a test chunk at each time-step to estimate the PE weights. Calls to the *DLS4LB* need to be inserted before and after the main calculations such that they are self-scheduled using DLS techniques as shown by lines in blue font color in Listing 1. In addition, steps for setting up and finalizing the *DLS4LB*, such as data allocation, deallocation and selecting the DLS technique, need to be added before and after the time-stepping loop (Lines 9 – 14), respectively.

The application needs to be a time-stepping application only to use the AWF technique. To use the *DLS4LB*, the application data need to be replicated among processes as the current implementation of the *DLS4LB* does not communicate the data required to compute the assigned chunk of loop iterations. It is the programmer’s responsibility to ensure that the data are available for computation and are communicated correctly. To use the extended version of the OpenMP runtime library, the application needs to be compiled with the GNU compilers, and the path to the extended library should be exported before execution.

3.2 Execution Each MPI rank (process) sends a work request to the master rank when it becomes free (Algorithm 1, Line 20) using the *DLS4LB*. In response, the master rank assigns a chunk of tasks to the requesting MPI rank. The size of the assigned chunk is determined by the employed DLS technique (specified in Algorithm 1, Line 8). *This allocated chunk at the MPI level is subsequently distributed to OpenMP threads for further scheduling and execution at the thread level.* Therefore, threads are assigned chunks (or sub-chunks of the chunk allocated at the MPI level) of tasks whenever they become free using *eLaPeSD*. Threads are assigned work until they complete the execution of the chunk allocated to their respective MPI rank. The process repeats until all tasks (N tasks) complete and `Main_calculations` of the current time-step is completed.

Algorithm 1: Two-level Dynamic Load Balancing via Self-scheduling

```
1 #include <mpi.h>
2 #include <omp.h>
3 #include "DLS4LB.h"
4 int main()
5 {
6 /* Application initialization*/
7 ...
8 DLS4LB_setup(P, N, DLS_method);
9 for  $l \leftarrow t_{init}$  to  $t_{final}$  do
10 | ...
11 | DLS4LB_Start_loop();
12 | Main_calculations();
13 | DLS4LB_End_loop();
14 | ...
15 DLS4LB_Finalize();
16 } /* End main */

17 void Main_calculations()
18 {
19 while ! DLS4LB_Terminated() do
20 | DLS4LB_Start_chunk(loop_start, loop_end);
21 | #pragma omp parallel for schedule(runtime)
22 | for  $i \leftarrow loop\_start$  to  $loop\_end$  do
23 | | /* Execute loop body */
24 | | ...
25 | DLS4LB_End_chunk();
26 } /* end main calculations*/
```

An application needs to be a time-stepping application to use the AWF technique. Otherwise, an application may use all other DLS techniques available in the *DLS4LB* library. The current implementation of the *DLS4LB* does not distribute application's data. Applications need to ensure that the data are available where the work is assigned either by replicating the data or communicating the data with work.

Calls to the dynamic load balancing libraries, such as *eLaPeSD* or *DLS4LB*, incur overhead, compared to using a static scheduling approach. This overhead is proportional to number of scheduling rounds and the cost of chunk calculation, which depends on the scheduling technique. In two-level dynamic load balancing, this overhead is proportional to the product of the number of scheduling rounds at each of the two levels. However, in severe load imbalance cases, this overhead is unavoidable and expected to be absorbed by the performance gain resulting from dynamic load balancing (c.f. Section 4).

4 Performance Evaluation and Discussion

Table 1: Details used in the design of factorial experiments for performance analysis.

Factors	Values	Properties
Applications	Mandelbrot (Mathematics)	$N = 0.6 \times 10^6$ tasks
	PSIA (Computer vision)	$N = 0.8 \times 10^6$ tasks
	SPHYNX (Astrophysics)	Test-case (1): Stellar collision, $N = 10.4 \times 10^6$ tasks Time-step: 6900
		Test-case (2a): Evrard collapse, $N = 1 \times 10^6$ tasks Time-step: 100, 500, 1000, 1700, 2000, 2300, 2500, 2800, full simulation[0 : 3000] Test-case (2b): Evrard collapse, $N = 1 \times 10^7$ tasks Time-step: 1
Two-level dynamic load balancing		
Thread-level self-scheduling	STATIC	Static: used as a baseline in this level
	SS, GSS, FSC*, TSS, FAC, RAND	Dynamic and nonadaptive
Process-level self-scheduling	NODLB	Static: used as a baseline at this level
	SS*, FSC*, mFSC, GSS, TSS, FAC, WF* AWF, AWF-B, -C, -D, -E, AF	Dynamic and adaptive
Computing systems	miniHPC	20 Dual socket Intel Broadwell nodes, 10 cores per socket, 64 GB RAM per node Two-level nonblocking fat-tree topology with Intel Omni-Path interconnection fabrics Network bandwidth: 100 Gbit/s, Network latency 100 nanoseconds
	Piz Daint	100 Cray XC50 single socket Intel Haswell nodes, 12 cores per socket, 64 GB RAM per node Dragonfly topology with Cray Aries routing and communications ASIC Network bandwidth: 150 Gbit/s, Network latency 130 nanoseconds

* DLS techniques implemented in the *eLaPeSD* or the *DLS4LB* libraries but not used in this work due to being unsuitable (SS, WF) or requiring profiling (FSC).

4.1 Design of Experiments Due to the multitude of factors and parameters that need to be considered for the experimental evaluation of the proposed two-level dynamic load balancing approach, we design the experiments as a set of factorial experiments. The details used in this design are included in Table 1.

4.1.1 Applications Mandelbrot is a computationally-intensive application which computes the Mandelbrot set [13] and generates its image. The application is parallelized such that the calculation of the value at every single pixel of a 2D image is a task, that is performed in parallel. To increase the variability between task execution times, the calculation is focused on the center of the image, i.e., the seahorse valley, where the computation is highly intensive. Mandelbrot is often used to evaluate the performance of dynamic scheduling techniques due to the high variation between its tasks execution times. Algorithm 2 shows the calculation of the Mandelbrot set for every pixel to generate a Mandelbrot set image. The for loop in Line 2 is parallelized with DLS techniques and the values of *start* and *end* are calculated based on the chunk size obtained by a DLS technique. The application computes the function $f_c(z) = z^4 + c$ instead of $f_c(z) = z^2 + c$ to increase the number of computations per task (see Lines 10-12). Line 9 represents the main source of load imbalance, as the number of repetitions of the calculations between Lines 9 to 14 is irregular.

The second application of interest is an application from the computer vision domain, namely the parallel spin-image algorithm (PSIA) [14]. PSIA converts a 3D object into a set of 2D descriptors (spin-images).

Algorithm 3 describes the steps of generating spin-images in PSIA and how it is parallelized. According to Algorithm 3, Lines 9 and 12, the amount of computations to generate spin-images is data-dependent and not identical over all the spin-images generated from the same object.

Algorithm 2: Mandelbrot set calculation

```
Inputs :  $W$ : image width
            $K$ : max iterations
            $RM$ : real max
            $Rm$ : real min
            $IM$ : image max
            $Im$ : image min
            $SR$ : scale real
            $SI$ : scale image
            $SC$ : scale color
            $data$ : pixel information

1  $N = 2$ 
  /* start and end are set by the scheduling technique according to the chunk
  size                                                                    */
  /* calculate pixels in parallel                                          */
2 for  $i = start \rightarrow end$  do
3    $z.real = z.imag = 0$ 
4    $rowID = i/W$ 
5    $colID = imodW$ 
6    $c.real = Rm + colID \times SR$ 
7    $c.imag = Im + (W - 1 - rowID) \times SI$ 
8    $k = 0$   $lengthsq = 0$ 
9   while  $lengthsq < (N \times N)$  do
10     $temp = z.real^4 - 6 \times z.imag^2 \times z.real^2 + z.imag^4 + c.real$ 
11     $z.imag = 4 \times z.real^3 \times z.imag - 4 \times z.real \times z.imag^3 + c.imag$ 
12     $z.real = temp$ 
13     $lengthsq = z.real^2 + z.imag^2$ 
14     $k ++$ 
15   $data[i] = (k - 1) \times SC$ 
```

This introduces an algorithmic source of load imbalance among the parallel processes generating the spin-images. The number of spin-images generated by each PE is governed by the **start** and **end** variables in Algorithm 3, Line 1, which is performed in parallel.

SPHYNX³ is a state-of-the-art production smoothed particle hydrodynamics (SPH) code [15]. It is also one of the few hydrodynamic codes in the literature that can simulate both Type Ia and core-collapse Supernovas, including nuclear reactions, neutrino transport, and general relativity correction terms. SPHYNX is a time-stepping application, parallelized using MPI and OpenMP. Each time-step consists of several computationally-intensive operations [15]. The workflow of SPHYNX is listed in Algorithm 4.

The performance of SPHYNX is studied for two simulation test-cases. The *stellar collision* test simulates the head-on impact of two Sun-like stars. This simulation has two independent

³Available at <http://astro.physik.unibas.ch/sphynx>

Algorithm 3: Spin-image calculation [27]

```
1 adCalculateSpinImages (W, B, S, OP, M, spinImages, start, end)
   Inputs : W: image width
             B: bin size
             S: support angle
             OP: list of oriented points
             M: number of oriented points
             spinImages: list of spin-images to be filled
2 for imageCounter = start → end do
3   P = OP[imageCounter]
4   tempSpinImage[W, W]
5   init(tempSpinImage)
6   for j = 0 → M do
7     X = OP[j]
8     npi = getNormal(P)
9     npj = getNormal(X)
10    if acos(npi · npj) ≤ S then
11       $k = \left\lceil \frac{W/2 - np_i \cdot (X - P)}{B} \right\rceil$ 
12       $l = \left\lceil \frac{\sqrt{\|X - P\|^2 - (np_i \cdot (X - P))^2}}{B} \right\rceil$ 
13      if  $0 \leq k < W$  and  $0 \leq l < W$  then
14        tempSpinImage[k, l]++
15    add(spinImages, tempSpinImage)
```

gravitating bodies and, therefore, the particle distribution is highly asymmetric. Second, the *Evrard collapse* is a common test used to examine the coupling between hydrodynamics and self-gravity in astrophysical codes. It simulates the collapse of an unstable cloud of gas and the formation of the subsequent shock-wave. This test is also studied on a large domain size (10 million particles) to explore its performance at large scale. These two test-cases offer a wide range of problem sizes, defined in the number of particles in the system and different particle distributions, that represent different load balancing challenges.

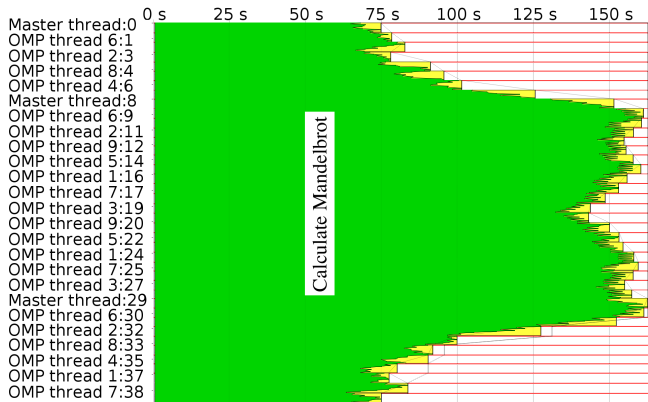
Figure 3 and Figure 4 show the load imbalance in the 3 applications of interest with no load balancing at the thread level and process level executing on miniHPC⁴. This load imbalance manifests as overhead (i.e., waiting time) as depicted in Figure 3 at the thread-level (yellow regions) and at the process-level (red regions). As calculating gravity is the most time-consuming computational step and also the most load imbalanced, this work focuses on improving the gravity calculation step of SPHYNX. To obtain representative performance measurements, the two-level

⁴ miniHPC is a fully controlled research and teaching HPC cluster at the Department of Mathematics and Computer Science at the University of Basel, Switzerland, <https://hpc.dmi.unibas.ch/HPC/miniHPC.html>.

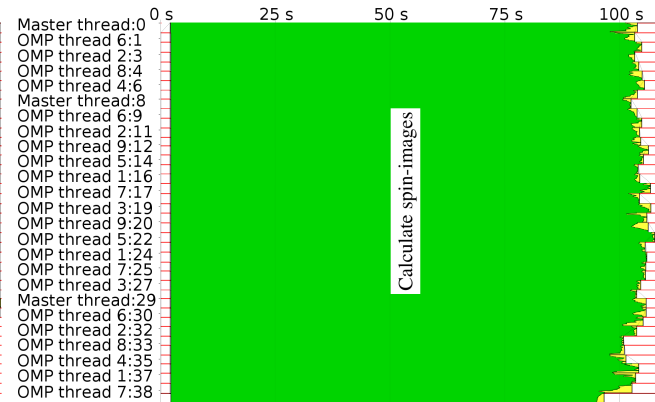
Algorithm 4: SPHYNX Computational Workflow

```
1 for  $l \leftarrow t_{init}$  to  $t_{final}$  do
2   1. Build tree
3   2. Find neighbors
4     2.1 Collective communication (number of neighbors)
5   3. Density & grad-h calculations
6     3.1 Collective communication (density & grad-h)
7   4. IAD calculations
8     4.1 Collective communication (IAD terms)
9   5. EOS &  $\nabla \mathbf{v}$  calculations
10    5.1 Collective communication ( $\nabla \cdot \mathbf{v}$  &  $\nabla \times \mathbf{v}$ )
11   6. Momentum & energy calculations
12    6.1 Collective communication ( $\nabla P$  &  $du/dt$ )
13   7. Gravity calculations
14    7.1 Collective communication (gravitational force and potential)
15   8. Update velocities, position, and energy
16   9. Time-step evaluation
17  10. Verification via conservation laws
```

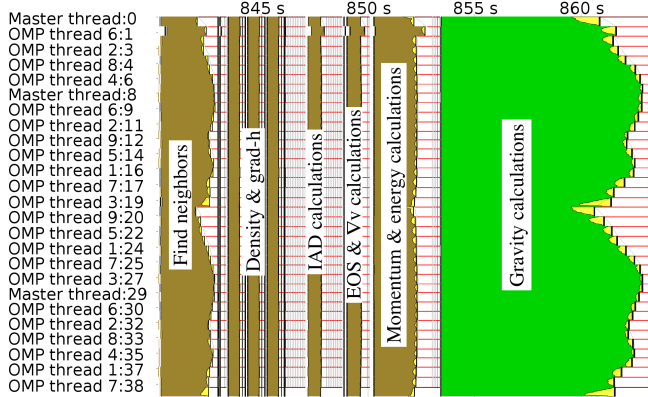
load balancing is tested in the middle of the simulation time (time-step 6900) for the *stellar collision* test-case. For the Evrard collapse test-case, all DLS combinations at the two levels are tested at multiple snapshots of the simulation as listed in Table 1. After testing all DLS combinations at different simulation stages, the identified best two-level DLS combination is used to execute the full simulation to measure the achieved overall performance improvement for a full SPH simulation. It is worth noting that the observed load imbalance in Figure 3 for a single time-step of SPHYNX can repeatedly be observed through the execution of the full SPH simulation, which typically requires 10^5 to 10^6 time-steps.



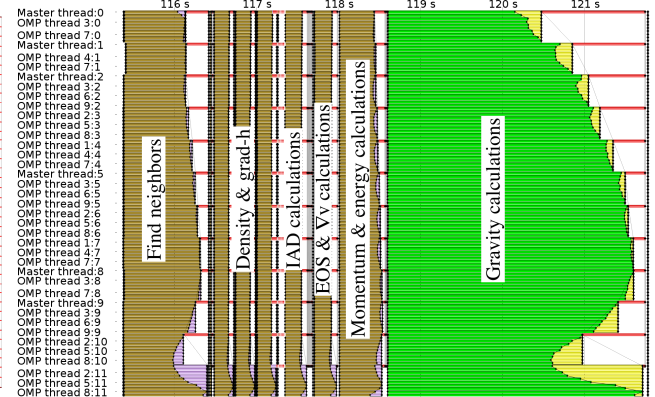
(a) Mandelbrot, 40 processes, 10 threads (miniHPC)



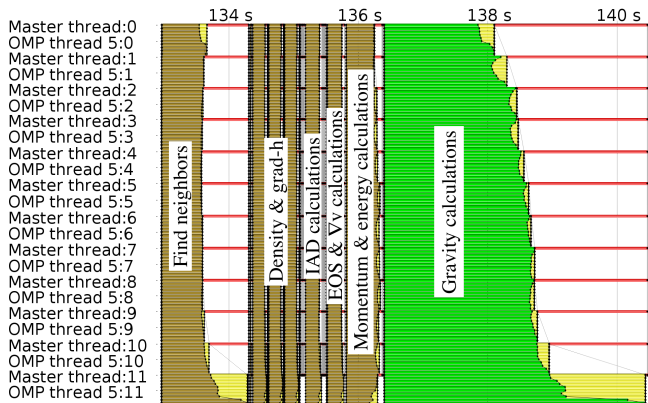
(b) PSIA, 40 processes, 10 threads (miniHPC)



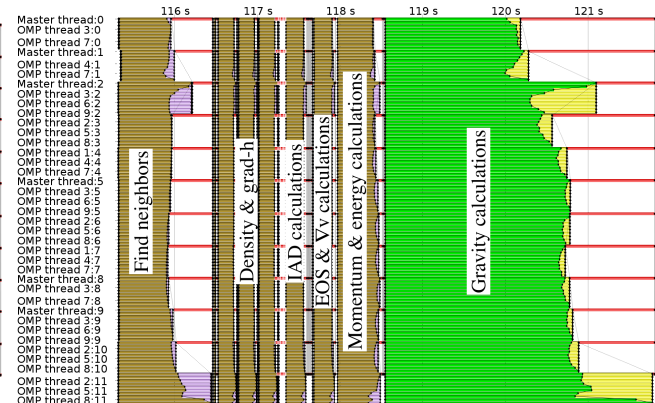
(c) Stellar collision time-step 6916, SPHYNX, 40 processes, 10 threads (miniHPC)



(d) Evrard, 1M particles, time-step 116, SPHYNX, 12 processes, 10 threads (miniHPC)

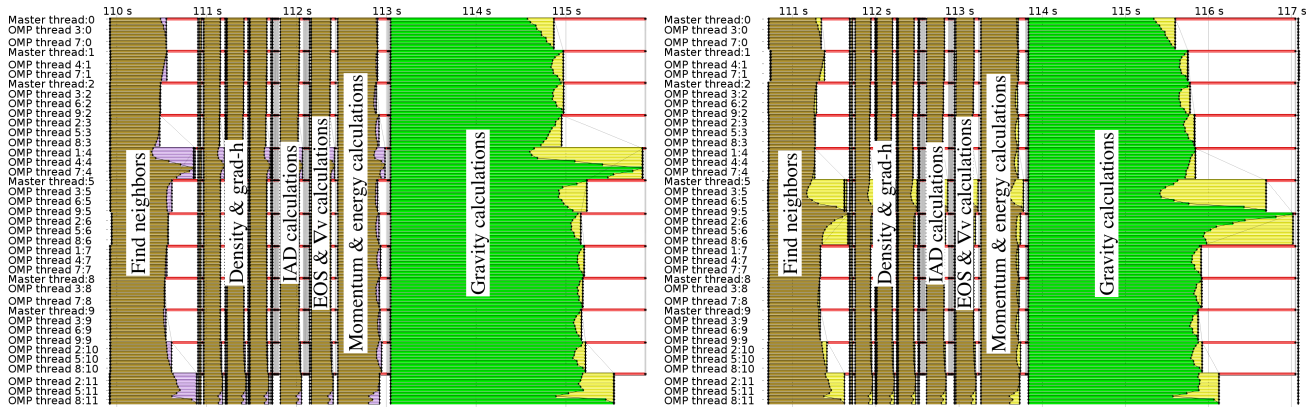


(e) Evrard, 1M particles, time-step 516, SPHYNX, 12 processes, 10 threads (miniHPC)

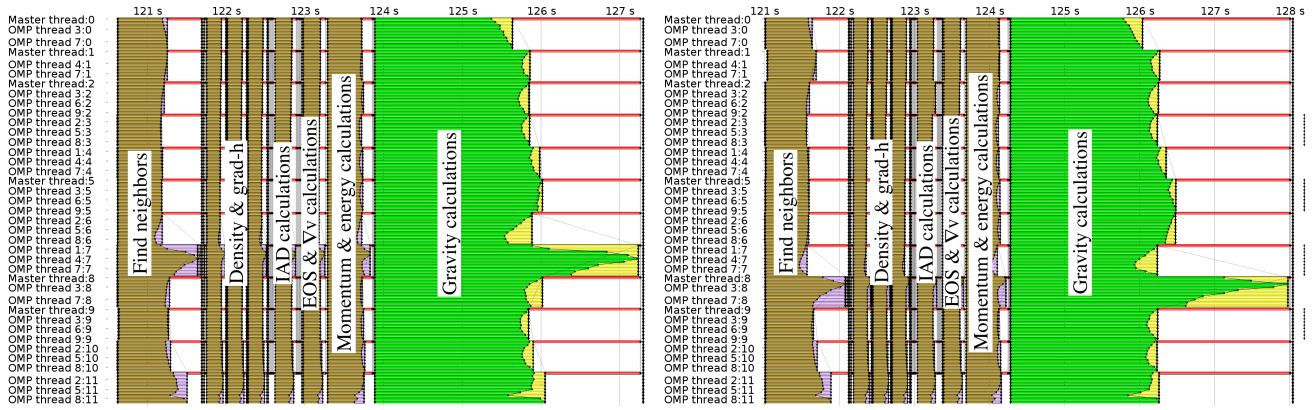


(f) Evrard, 1M particles, time-step 1016, SPHYNX, 12 processes, 10 threads (miniHPC)

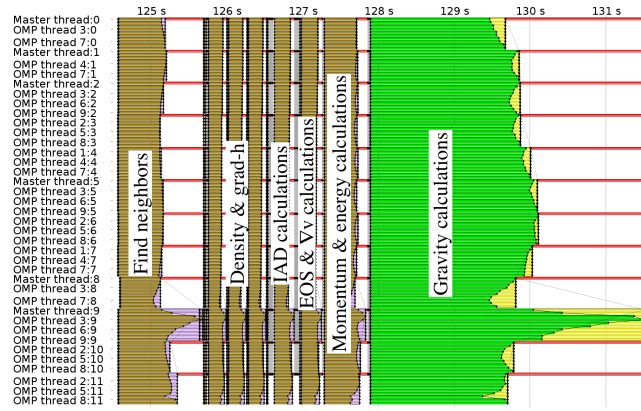
Figure 3: Impact of two-level load imbalance at thread level and process level in the three scientific applications. Idle time due to load imbalance is shown in yellow at the thread level and in red at the process level. We apply DLS for each application to the load imbalance in their respective green regions.



(a) Evrard, 1M particles, time-step 1716, SPHYNX, 12 processes, 10 threads (miniHPC) (b) Evrard, 1M particles, time-step 2016, SPHYNX, 12 processes, 10 threads (miniHPC)



(c) Evrard, 1M particles, time-step 2316, SPHYNX, 12 processes, 10 threads (miniHPC) (d) Evrard, 1M particles, time-step 2516, SPHYNX, 12 processes, 10 threads (miniHPC)



(e) Evrard, 1M particles, time-step 2816, SPHYNX, 12 processes, 10 threads (miniHPC)

Figure 4: Impact of two-level load imbalance at thread level and process level in the Evrard collapse test-case, 1M particles, with SPHYNX. Idle time due to load imbalance is shown in yellow at the thread level and in red at the process level level. We apply DLS to the load imbalance in their green region corresponding to gravity calculations.

4.1.2 Two-level dynamic load balancing Six loop scheduling techniques are considered at the thread level via the *eLaPeSD* OpenMP library and eleven loop scheduling techniques at the process level via the *DLS4LB*, yielding a combination of $6 \times 11 = 66$ experiments per application or test-case. FSC technique is not considered in this work neither at the thread level nor the process level as it requires the profiling of the application to estimate the standard deviation of task execution times σ and the scheduling overhead h . Application performance with FSC is significantly influenced by the provided σ and h values.

The SS technique is not considered at the process level, as it assigns a single task to a requesting process, which waste the thread level parallelism as only one thread is used. WF technique is not used in this work as well, as it is designed for heterogeneous computing systems, which is not the case for miniHPC. AWF technique is only used with SPHYNX as it learns PE relative performance weights from previous time-steps. NODLB and STATIC denote the scenario where application tasks are statically and equally divided among the processes or threads, respectively.

A minimum chunk size is specified at the process level to avoid processes being assigned a very small chunk of tasks towards the end of the execution, which could not contain enough work to distribute to threads within a process and increase the scheduling rounds and consequently the overall scheduling overhead. The minimum chunk size at the process level is set to half the chunk size of mFSC technique, that is 532, 700, 7278, 2549, for Mandelbrot, PSIA, SPHYNX with stellar collision test, and SPHYNX with Evrard collapse test, respectively. At the thread level the minimum chunk size is set to 1 (OpenMP default) as the scheduling overhead is small and to achieve the best possible load balance.

4.1.3 Computing systems The proposed is tested on miniHPC and Piz Daint⁵. Each MPI rank is pinned to a CPU socket of miniHPC, to improve the data locality among threads within an MPI rank. The number of threads per MPI rank is set to be equal to the number of cores per socket. Therefore, each compute node of miniHPC executes two MPI ranks, one per socket, with 10 OpenMP threads within each MPI rank. In addition, we use Piz Daint to run large scale experiments with 100 nodes and 12 threads per node for the execution of Evrard collapse test-case with 10 million particles. In all experiments, a rank is pinned to a processor socket within a compute node, i.e., two ranks per node on miniHPC and one rank per node on Piz Daint.

4.2 Experimental Results The performance results of the three scientific applications of interest are depicted in Figure 5, Figure 6 and Figure 7. The figures show the parallel execution time of Mandelbrot and PSIA and the computing time of the gravity per time-step for SPHYNX. Figure 5 shows the performance percent improvement with DLS techniques normalized to not using any dynamic load balancing mechanism in any of the thread level or the process level (NODLB_STATIC).

Using two-level load balancing improved the performance of Mandelbrot up to 21% as shown in Figure 5a with TSS at the process level and SS at the thread level. The performance improvement is much lower in PSIA than in Mandelbrot as PSIA is mildly imbalanced as shown in Figure 3b. Two-level load balancing improved the performance of gravity calculations in

⁵Piz Daint is a Cray XC50 supercomputer system, the Swiss National Supercomputing Center (CSCS), <https://www.cscs.ch/computers/dismissed/piz-daint-piz-dora/>.

SPHYNX also by 11% for stellar collision test-case in Figure 5c with AWF-C at the process level and FAC at the thread level and by 43% for Evrard collapse test-case, $1M$ particles, in Figure 5e with GSS at the process level and FAC at the thread level.

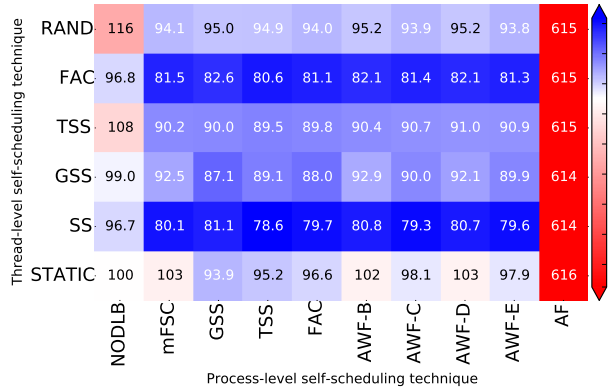
The best two-level DLS combination for the gravity part of Evrard collapse, namely GSS+FAC, also holds when we increase problem size to $10M$ particles. GSS+FAC is the most efficient combination at the two levels on 100 nodes and 12 threads per node on Piz Daint and improves SPHYNX performance (gravity part) by 11% (Figure 6f). The relatively low performance improvement for the large-scale experiments is attributed to the fact that they are performed from the beginning of the astrophysical simulation, i.e., time-step 1, where computation and load imbalance are less intensive. The RAND technique is excluded from these large scale experiments due to its poor performance on the Evrard collapse test with $1M$ particles. We plan to perform additional experiments (snapshots into the middle of the simulation and full simulation) for the Evrard collapse (gravity part and entire application) with $10M$ particles on Piz Daint similar to the Evrard collapse with $1M$ particles on miniHPC.

In general, FAC result in the best performance at the thread level while GSS and AWF variants result in the best performance at the process level. SS results in poor performance for SPHYNX at the thread level due to the fine granularity of its tasks (240 μ s on average). At the process level, the AF technique performs poorly for the experiments conducted in this work. This can be attributed in part to its large overhead and the lack of high variability (in application and computing system) to hide this overhead and benefit from AF. Specifically, the AF technique is designed for highly irregular workloads that execute in stochastic environments. The experiments conducted in this work have insufficient variability to justify the adjustments of AF.

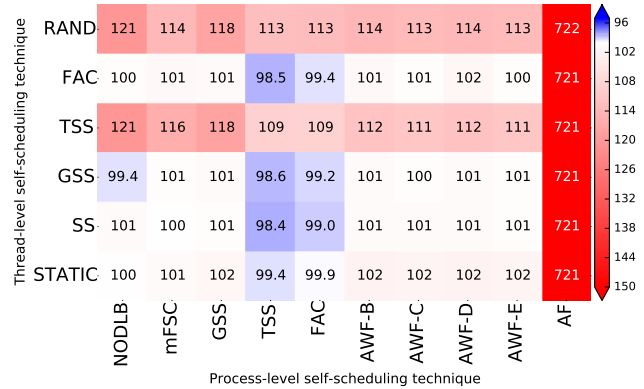
Figure 7 shows the best average parallel execution time over 20 repetitions (Mandelbrot and PSIA) or time-step (SPHYNX) when: (1) Using no load balancing at any of the two levels; (2) Using the best DLS technique only at the thread level; (3) Using the best DLS technique only at the process level; (4) Using the best available combination of DLS techniques at the thread level and the process level. The results in Figure 7 show the benefits of two-level load balancing versus only one-level as conceptually illustrated in Figure 2. The results show that certain performance gains are achieved by single-level load balancing (either thread level or process level middle boxes) as predicted by Figure 2, however, the best performance is always achieved by two-level dynamic load balancing.

GSS and FAC was identified as the best combination of DLS techniques at the process level and the thread level, respectively, by testing all 66 DLS combinations at the two levels for Evrard collapse test-case, $1M$ particles, at different stages of the simulation at time-steps 100, 500, 1000, 1700, 2000, 2300, 2500, and 2800.

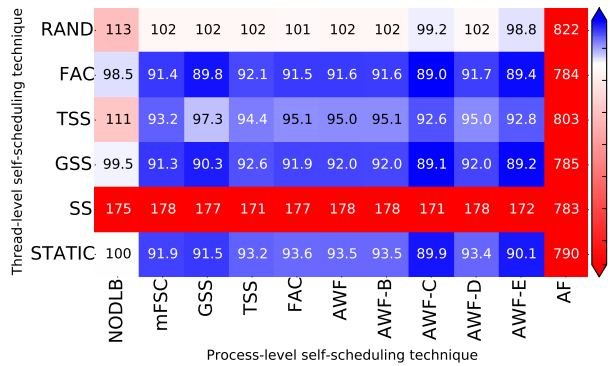
Figure 8 shows the parallel execution time per time-step for the full simulation of Evrard collapse with $1M$ particles on miniHPC. The results show that time-step execution time with two-level dynamic load balancing is always better than the baseline with no load balancing at the two levels and lead to an overall application performance improvement of 15%.



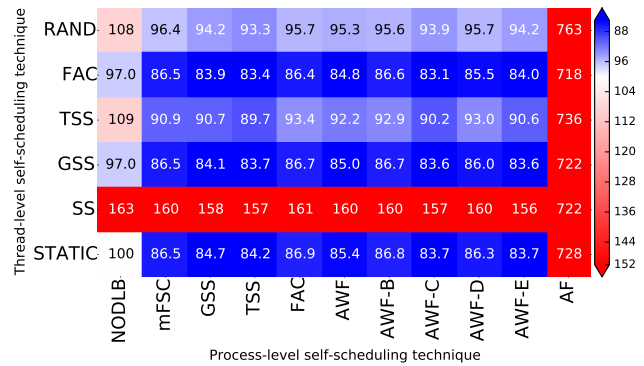
(a) Mandelrot, 40 processes, 10 threads (miniHPC)



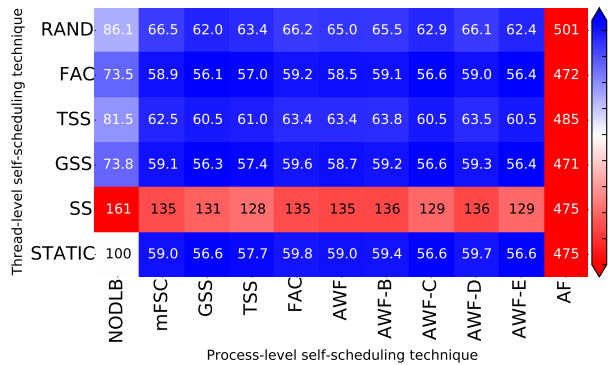
(b) PSIA, 40 processes, 10 threads (miniHPC)



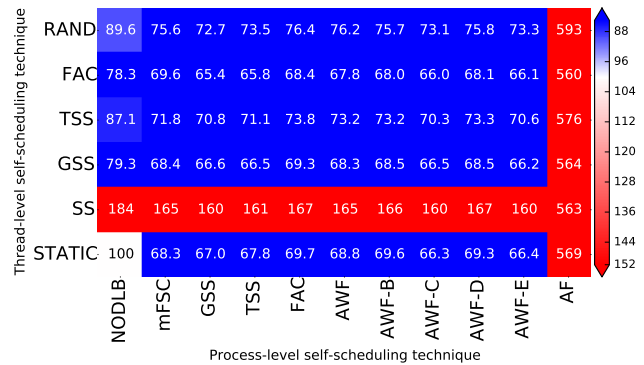
(c) Stellar collision time-step 6900-6920, 40 processes, 10 threads (miniHPC)



(d) Evrard collapse, 1M particles, time-step 100-120, 12 processes, 10 threads (miniHPC)

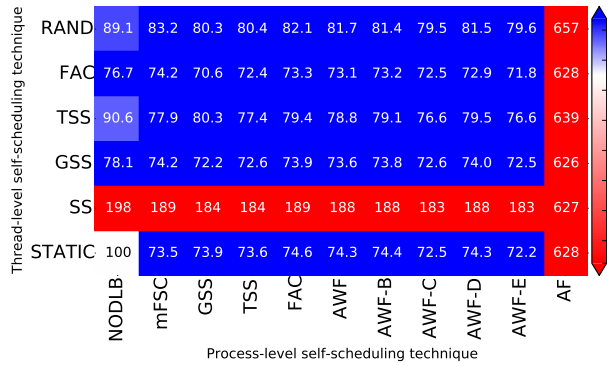


(e) Evrard collapse, 1M particles, time-step 500-520, 12 processes, 10 threads (miniHPC)

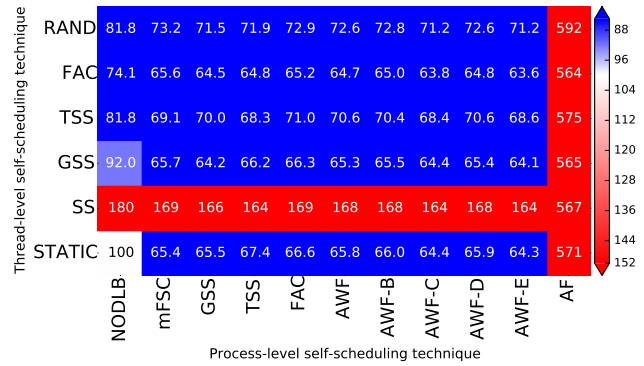


(f) Evrard collapse, 1M particles, time-step 1000-1020, 12 processes, 10 threads (miniHPC)

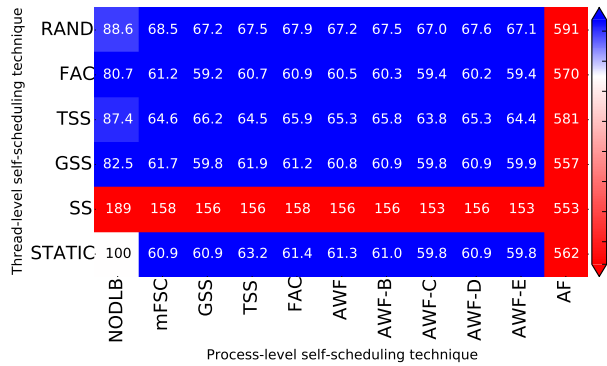
Figure 5: Impact of the two-level dynamic load balancing on the performance of the three scientific applications. Percent improvement corresponds to the average of 20 repetitions or time-steps with two-level load balancing normalized with respect to NODLB_STATIC. White, red and blue correspond to baseline, degraded and improved performance, respectively.



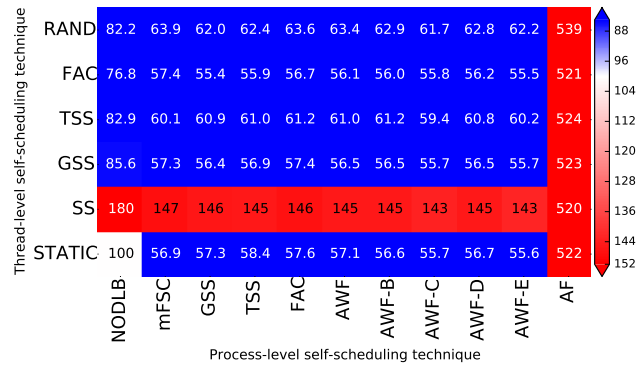
(a) Evrard collapse, 1M particles, time-step 1700-1720, 12 processes, 10 threads (miniHPC)



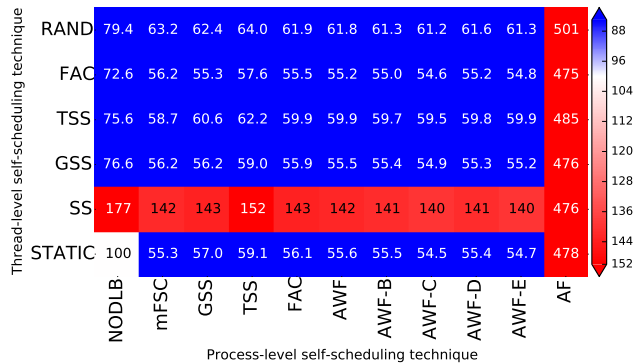
(b) Evrard collapse, 1M particles, time-step 2000-2020, 12 processes, 10 threads (miniHPC)



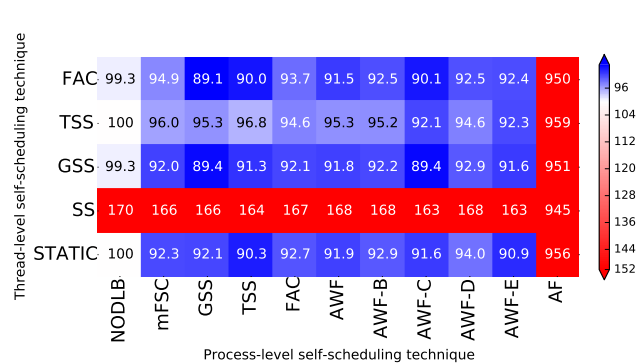
(c) Evrard collapse, 1M particles, time-step 2300-2320, 12 processes, 10 threads (miniHPC)



(d) Evrard collapse, 1M particles, time-step 2500-2520, 12 processes, 10 threads (miniHPC)

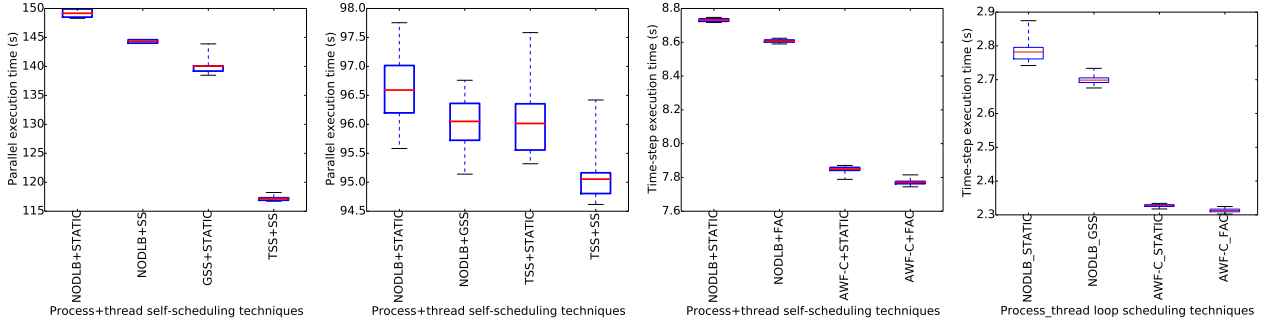


(e) Evrard collapse, 1M particles, time-step 2800-2820, 12 processes, 10 threads (miniHPC)

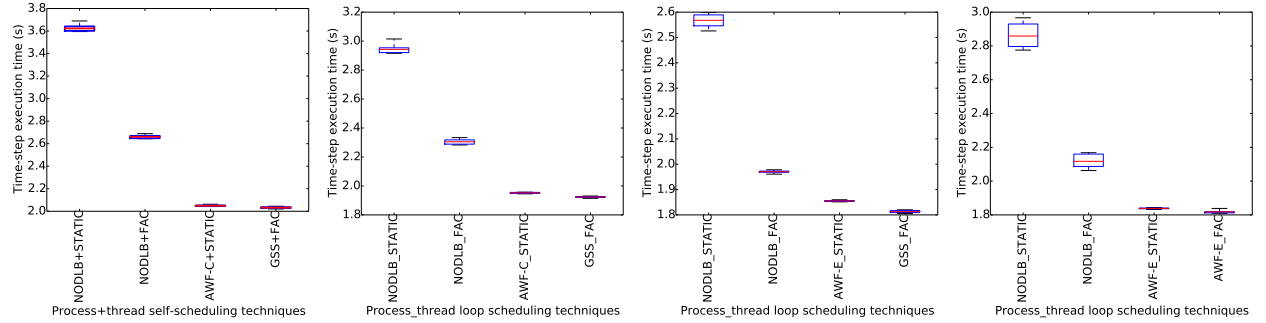


(f) Evrard collapse (gravity) 10M particles, time-steps 1-20, 100 processes, 12 threads (Piz Daint)

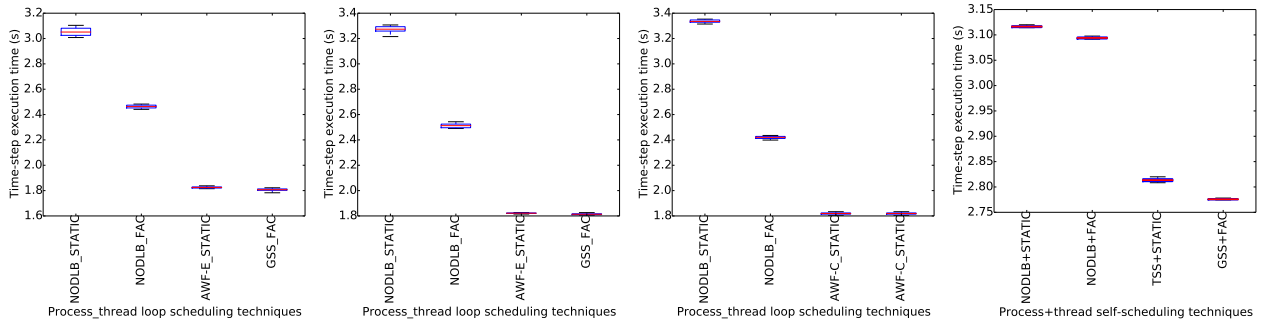
Figure 6: Impact of the two-level dynamic load balancing on the performance of the Evrard collapse test-case, 1M and 10M particles, with SPHYNX. Percent improvement corresponds to the average of 20 repetitions or time-steps with two-level load balancing normalized with respect to NODLB_STATIC. White, red and blue correspond to baseline, degraded and improved performance, respectively.



(a) Mandelbrot, 40 processes, 10 threads (miniHPC) (b) PSIA, 40 processes, 10 threads (miniHPC) (c) Stellar collision, 10M particles, time-step 6900-6920, 12 processes, 10 threads (miniHPC) (d) Evrard collapse, 1M particles, time-step 100-120, 12 processes, 10 threads (miniHPC)



(e) Evrard collapse, 1M particles, time-step 500-520, 12 processes, 10 threads (miniHPC) (f) Evrard collapse, 1M particles, time-step 1000-1020, 12 processes, 10 threads (miniHPC) (g) Evrard collapse, 1M particles, time-step 1700-1720, 12 processes, 10 threads (miniHPC) (h) Evrard collapse, 1M particles, time-step 2000-2020, 12 processes, 10 threads (miniHPC)



(i) Evrard collapse, 1M particles, time-step 2300-2320, 12 processes, 10 threads (miniHPC) (j) Evrard collapse, 1M particles, time-step 2500-2520, 12 processes, 10 threads (miniHPC) (k) Evrard collapse, 1M particles, time-step 2800-2820, 12 processes, 10 threads (miniHPC) (l) Evrard collapse (gravity), 10M particles, time-steps 1-12, 20 processes, 100 threads (Piz Daint)

Figure 7: Impact of single and two-level dynamic load balancing on the execution time of the three scientific applications. Each plot shows in the following order: the execution time with the baseline (NODLB_STATIC), best DLS technique at thread level, best DLS technique at process level, and best two-level combination. The red line represents the average performance over 20 repetitions or time-steps, the boxes define the first and third quartiles, and the whiskers are maximum and minimum values.

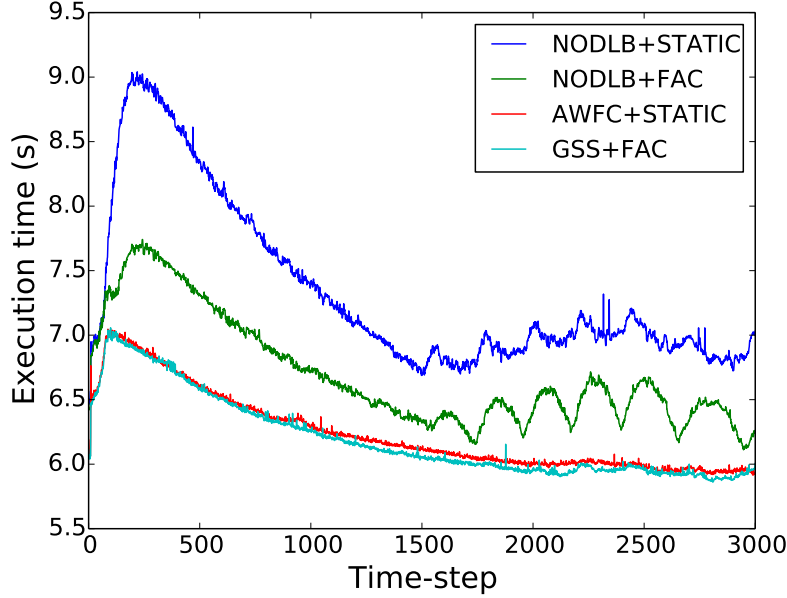


Figure 8: Time-step execution time of Evrard collapse test-case, $1M$ particles, in SPHYNX with 12 processes and 10 threads per process on miniHPC. The two-level dynamic load balancing improved the performance of SPHYNX throughout the full simulation, achieving 15% overall improvement in execution time.

4.3 Discussion Execution traces in Figure 3 show different profiles of two-level load imbalance. The Mandelbrot execution trace in Figure 3a shows a severe case of two-level load imbalance, where there is high variability in processes finishing times, and in threads finishing times within a single process, as demonstrated in Figure 1. single-level load balancing (thread level or process level) in this case achieves limited performance improvement as predicted in Figure 2 and confirmed by experimental results in Figure 7a, which showed the significant improvement of performance with two-level dynamic load balancing versus its slight improvement with single-level load balancing. While Mandelbrot represents an extreme load imbalance, PSIA represents the other extreme, where processes and threads within a process are slightly imbalanced as shown in Figure 3b. Therefore, the maximum achievable performance improvement in PSIA is much smaller (1.5%) than that in Mandelbrot (21%).

SPHYNX execution in stellar collision execution suffers from high load imbalance at the process level and low load imbalance at the thread level as shown in Figure 3c. This is reflected by the slight effect of thread level load balancing and the significant impact of process level load balancing in improving its performance, as shown in Figure 7c. For the Evrard collapse, $1M$ particles, however, one can observe a severe load imbalance at the process level. This load imbalance at the process level is in fact caused by two threads lagging the execution of the last process behind all other processes as can be seen in Figure 3e. In this case, thread level load balancing not only improves the load balancing at the thread level but also at the process level as the last process will finish early, making it closer to the other processes finishing times.

Alternatively, process level load balancing will also distribute the high workload of the last two threads among all the processes, therefore, dissolving the thread level load imbalance among processes. This is confirmed by the significant performance improvement by both thread level alone and process level alone in Figure 7e. This represents an interesting case where load balancing from the thread level propagates to the process level and vice versa.

Another important observation from Figure 7 is that the best combination of DLS techniques at the thread level and process level (fourth column), is not always the combination of the best technique at the thread level (second column) and the best technique at the process level (third column). These show the interplay between the thread level and the process level load balancing, as load balancing at one level changes the load imbalance at the other level. As illustrated in Figure 2 the load balancing techniques are needed at both levels in the right combination, to achieve the best balanced load execution.

5 Conclusion and Future Work

In this work, load imbalance at the thread level and process level of three scientific applications, has been analyzed. Load imbalance degrades performance, adversely affects scalability, and becomes more significant as the number of processes increases. Dynamic load balancing via self-scheduling has been used in this work to address the two-level load imbalance and improve scientific applications performance. *eLaPeSD* has been used to employ DLS at the thread level and the *DLS4LB* at the process level. In addition, the *DLS4LB* has been extended with the AWF technique that is specifically designed for time-stepping scientific applications, such as SPHYNX. The proposed two-level load balancing approach using the *DLS4LB* and the *eLaPeSD* is *generic* and can be applied to any MPI+OpenMP application. Based on the nature of the load imbalance at the thread level and process level, certain performance improvements can be achieved with single-level load balance either at the thread level or the process level. However, the best application performance can only be achieved by addressing load imbalance *jointly* at the two-levels. Also, the DLS techniques at thread level and process level influence each other, and this influence should not be ignored. In certain cases, load balancing at thread level propagates to the process level and vice versa. In addition, the best performing two-level combination is not always the combination of the two best performing DLS techniques at a single level alone. This highlights the interplay between thread level and process level load balancing, as load balancing at one level changes the load imbalance at the other level.

The extension of the *DLS4LB* to work with distributed data as well as replicated data is planned in the future. In addition, implementing self-scheduling techniques using decentralized control approach to improve their scalability is also envisioned in the future. Also, an intelligent selection of the best combination of thread level and process level scheduling techniques using simulation or machine learning is planned as future work.

Acknowledgment

This work has been partially supported by the Swiss Platform for Advanced Scientific Computing (PASC) project SPH-EXA: Optimizing Smooth Particle Hydrodynamics for Exascale Computing and by the Swiss National Science Foundation in the context of the “Multi-level Scheduling in Large Scale High Performance Computers” (MLS) grant, number 169123.

References

- [1] F. M. Ciorba, C. Iwainsky, and P. Buder, "OpenMP Loop Scheduling Revisited: Making a Case for More Schedules," in *Proceedings of the 2018 International Workshop on OpenMP*, September 2018.
- [2] A. Mohammed and F. M. Ciorba, "Research Report - University of Basel, Switzerland." <https://drive.switch.ch/index.php/s/aaqAdp3X2Fxsoe>, October 2018. [Online; accessed 19 Oct 2018].
- [3] H. Jin, D. Jespersen, P. Mehrotra, R. Biswas, L. Huang, and B. Chapman, "High Performance Computing Using MPI and OpenMP on Multi-core Parallel Systems," *Parallel Computing*, vol. 37, no. 9, pp. 562–575, 2011.
- [4] R. Rabenseifner, G. Hager, and G. Jost, "Hybrid MPI/OpenMP Parallel Programming on Clusters of Multi-core SMP Nodes," in *17th Euromicro International Conference on Parallel, Distributed and Network-based Processing*, pp. 427–436, 2009.
- [5] L. Smith and M. Bull, "Development of Mixed Mode MPI/OpenMP Applications," *Scientific Programming*, vol. 9, no. 2-3, pp. 83–98, 2001.
- [6] B. D. Kandhai, "Large Scale Lattice-Boltzmann Simulations," *Thesis University of Amsterdam*, 1999.
- [7] H. Menon, L. Wesolowski, G. Zheng, P. Jetley, L. Kale, T. Quinn, and F. Governato, "Adaptive Techniques for Clustered N-Body Cosmological Simulations," *Computational Astrophysics and Cosmology*, vol. 2, no. 1, p. 1, 2015.
- [8] S. Bak, H. Menon, S. White, M. Diener, and L. Kale, "Multi-Level Load Balancing with an Integrated Runtime Approach," in *2018 18th IEEE/ACM International Symposium on Cluster, Cloud and Grid Computing (CCGRID)*, pp. 31–40, IEEE, 2018.
- [9] A. Eleliemy, A. Mohammed, and F. M. Ciorba, "Exploring the Relation Between Two Levels of Scheduling Using a Novel Simulation Approach," in *Proceedings of 16th International Symposium on Parallel and Distributed Computing*, p. 8, July 2017.
- [10] I. Banicescu and V. Velusamy, "Load Balancing Highly Irregular Computations with the Adaptive Factoring," in *the 16th International Parallel and Distributed Processing Symposium Workshops*, p. 195, IEEE, 2002.
- [11] R. L. Cariño and I. Banicescu, "Dynamic Load Balancing with Adaptive Factoring Methods in Scientific Applications," *Journal of Supercomputing*, vol. 44, no. 1, pp. 41–63, 2008.
- [12] I. Banicescu and S. F. Hummel, "Balancing Processor Loads and Exploiting Data Locality in N-Body Simulations," in *Proceedings of the ACM/IEEE International Conference for High Performance Computing, Networking, Storage, and Analysis*, p. 43, December 1995.
- [13] B. B. Mandelbrot, "Fractal Aspects of the Iteration of $Z \rightarrow \Lambda z (1-Z)$ for Complex Λ and Z ," *Annals of the New York Academy of Sciences*, vol. 357, no. 1, pp. 249–259, 1980.
- [14] A. Eleliemy, M. Fayze, R. Mehmood, I. Katib, and N. Aljohani, "Load Balancing on Parallel Heterogeneous Architectures: Spin-image Algorithm on CPU and MIC," in *Proceedings of the 9th EUROSIM Congress on Modelling and Simulation*, pp. 623–628, September 2016.
- [15] R. M. Cabezón, D. Garcia-Senz, and J. Figueira, "SPHYNX: An Accurate Density-based SPH Method for Astrophysical Applications," *Astronomy & Astrophysics*, vol. 606, p. A78, 2017.
- [16] R. D. Blumofe and C. E. Leiserson, "Scheduling Multithreaded Computations by Work Stealing," *Journal of the ACM*, vol. 46, no. 5, pp. 720–748, 1999.
- [17] T. Peiyi and Y. Pen-Chung, "Processor Self-Scheduling for Multiple-Nested Parallel Loops," in *Proceedings of the International Conference on Parallel Processing*, pp. 528–535, 1986.

- [18] C. P. Kruskal and A. Weiss, "Allocating Independent Subtasks on Parallel Processors," *IEEE Transactions on Software Engineering*, vol. SE-11, no. 10, pp. 1001–1016, 1985.
- [19] I. Banicescu, F. M. Ciorba, and S. Srivastava, *Scalable Computing: Theory and Practice*, ch. Performance Optimization of Scientific Applications using an Autonomic Computing Approach, pp. 437–466. No. 22, John Wiley & Sons, Inc, 2013.
- [20] C. D. Polychronopoulos and D. J. Kuck, "Guided Self-Scheduling: A Practical Scheduling Scheme for Parallel Supercomputers," *IEEE Transactions on Computers*, vol. 100, no. 12, pp. 1425–1439, 1987.
- [21] T. H. Tzen and L. M. Ni, "Trapezoid Self-scheduling: A Practical Scheduling Scheme for Parallel Compilers," *IEEE Transactions on Parallel and Distributed Systems*, vol. 4, no. 1, pp. 87–98, 1993.
- [22] S. Flynn Hummel, E. Schonberg, and L. E. Flynn, "Factoring: A Method for Scheduling Parallel Loops," *Communications of the ACM*, vol. 35, no. 8, pp. 90–101, 1992.
- [23] S. Flynn Hummel, J. Schmidt, R. N. Uma, and J. Wein, "Load-sharing in Heterogeneous Systems via Weighted Factoring," in *Proceedings of the Annual ACM Symposium on Parallel Algorithms and Architectures*, pp. 318–328, 1996.
- [24] I. Banicescu, V. Velusamy, and J. Devaprasad, "On the Scalability of Dynamic Scheduling Scientific Applications With Adaptive Weighted Factoring," *Cluster Computing*, vol. 6, no. 3, pp. 215–226, 2003.
- [25] I. Banicescu and Z. Liu, "Adaptive Factoring: A Dynamic Scheduling Method Tuned to the Rate of Weight Changes," in *Proceedings of the High Performance Computing Symposium*, pp. 122–129, 2000.
- [26] R. L. Carino and I. Banicescu, "A Tool for a Two-level Dynamic Load Balancing Strategy in Scientific Applications," *Scalable Computing: Practice and Experience*, vol. 8, no. 3, 2007.
- [27] A. Eleliemy, A. Mohammed, and F. M. Ciorba, "Efficient Generation of Parallel Spin-images Using Dynamic Loop Scheduling," in *Proceedings of the 19th IEEE International Conference for High Performance Computing and Communications Workshops*, pp. 34–41, 2017.
- [28] D. H. Bailey, "Nas parallel benchmarks," *Encyclopedia of Parallel Computing*, pp. 1254–1259, 2011.
- [29] S. Che, M. Boyer, J. Meng, D. Tarjan, J. W. Sheaffer, S.-H. Lee, and K. Skadron, "RODINIA: A Benchmark Suite for Heterogeneous Computing," in *IEEE International Symposium on Workload Characterization*, pp. 44–54, 2009.
- [30] M. Lieber and W. E. Nagel, "Highly Scalable SFC-based Dynamic Load Balancing and its Application to Atmospheric Modeling," *Future Generation Computer Systems*, vol. 82, pp. 575–590, 2018.
- [31] S. K. Gutiérrez, *Adaptive Parallelism for Coupled, Multithreaded Message-Passing Programs*. PhD thesis, University of New Mexico, 2018.
- [32] H. Menon, N. Jain, G. Zheng, and L. Kale, "Automated load balancing invocation based on application characteristics," in *Cluster Computing (CLUSTER), 2012 IEEE International Conference on*, pp. 373–381, IEEE, 2012.
- [33] Y. Wang, Y. Zhang, Y. Su, X. Wang, X. Chen, W. Ji, and F. Shi, "An Adaptive and Hierarchical Task Scheduling Scheme for Multi-core Clusters," *Parallel computing*, vol. 40, no. 10, pp. 611–627, 2014.